Supporting information

A linearly programmable strategy for polymer elastomer mechanics

Dichang Xue, Xing Su*, Jin Xu, Xiaodong Li, Hao jiang, Lichen Zhang, Zichen Bai, Ruibin Wang, Zitong Deng, Lixiang Zhu, Zhengnan Su, Meishuai Zou*

School of Materials Science and Engineering, Beijing Institute of Technology, No. 5 South Zhongguancun Street, Haidian District, Beijing, 100081, China

*corresponding author, e-mail: sx1020@126.com (X. Su), zoums@bit.edu.cn

Table of contents:

Supplementary Text

MATERIALS AND METHODS

MATERIALS

Isophorone diisocyanate (IPDI) and triethylamine (TEA) were bought from Shanghai Aladdin Biochemical Technology Co., Ltd. Aluminium nitrate nonahydrate, Aluminium nitrate hydrate pure water ($AlNO_3 \cdot 9H_2O$) diphenylmethane diisocyanate (MDI), Polytetrahydrofuran (PTMG2000), 1,4-butanediol (BDO), and anhydrous ethanol were purchased from Shanghai Macklin Biochemical Technology Co., Ltd. Dopamine hydrochloride (DA) was supplied by Descartes Daily Chemical Co., Ltd. *N*-*N*′-dimethylformamide (DMF) and tetrahydrofuran (THF) were supplied by Meryer Technologies Co., Ltd. All of the above materials were analytically pure, and used as received.

Synthesis of AlPU, BPU and APU

The synthesis of the BPU material was shown below. 80g PTMG was added into a three-neck flask, which was heated up to 120° C and stirred for 4 hours in vacuum to remove water. Afterwards, dehydrated PTMG (40 g, 20 mmol), MDI (10.0104 g, 40 mmol), BDO (1.8024 g, 20mmol), DBTDL (0.0508 g, 0.0852mmol) and DMF (150 ml) were added into PTMG with constant stirring (stirring speed: 200 r/min) for 7 hours at 80℃ in order to achieve complete dissolution. After reaction, the solution was treated by anhydrous ethanol and the white precipitate was dried and collected for obtaining the MPU material.

The synthesis of the AlPU material was shown as follows. Dehydrated PTMG (40 g, 20 mmol), IPDI (8.8916 g, 40 mmol) and DMF (100 ml) were well mixed. The temperature was then raised to, and the reaction was carried out at 80℃ under constant stirring (stirring speed: 200 r/min) for 6 hours to obtain the IPDI-terminated PTMG prepolymer. Dopamine hydrochloride (7.5856 g, 40 mmol) and TEA (4.0476 g, 40 mmol) were mixed ultrasonically and then added into the prepolymer solution. The temperature was lowered to 50℃ and the reaction carried on for another 24 hours

for obtaining the dopamine-terminated polymer chains. The obtained solution was washed with deionized water and viscous product was precipitated and collected. Aluminium nitrate hydrate (5.0017 g, 13.3 mmol) was introduced and the transparent AlPU polymer film was obtained via dehydration in the hot (80℃) oven for 24 hours. Fe^{3+}, Cu^{2+}, Ni^{2+} and Ca^{2+} were also tried to serve as chelating agent instead of Al^{3+}, which were abbreviated as FePU, CuPU, NiPU and CaPU, respectively.

The typical synthetic routes for the APU described in detail as follows. A three-neck round bottom flask equipped with a mechanical stirrer was charged with PTMEG (Mn of 2000 g mol^{-1}, 10.0 g) followed by heating at 110 ℃ under vacuum and stirring for 30 min to remove the moisture. After cooling the reaction system to 80 ℃, the mixture of diisocyanate [IPDI (2.22 g, 10 mmol)] and dibutyltin dilaurate (DBTDL, 0.02 g) dissolved in *N-N'*-dimethylacetamide (DMAc, 5 mL) was added into the flask. The reaction system was further heated at 80 °C under N2 atmosphere and stirring for 3 h, followed by being cooled to 40 °C. Consequently, AD (0.87 g, 5 mmol) as the chain extender, dissolved in DMAc (60 mL), was added into the reaction system that was further kept at 40 ℃ for 15 h under stirring and N_2 atmosphere. Viscous and transparent solutions of the APU polymers were finally obtained. The as-obtained polymer solutions were finally poured into glass petri dishes and then heated on a hot plate at 85 ℃ overnight, followed by drying at 80 ℃ for 48 h under vacuum to obtain the elastomer samples.

The synthesis of AlPU/BPU hybrid materials was shown as follows. The AlPU and BPU samples were weighed according to a certain mass ratio (1:9, 2:8, 3:7, 4:6, 5:5, or 6:4, more details could be found in **Table S1**). The AlPU and BPU samples were dissolved and mixed by THF at the total solid concentration of 23.07 wt%. The derived AlPU/BPU solutions were dried for obtaining the AlPU/BPU materials following the same method as discussed above. The derived AlPU/BPU materials were referred as x-AlPU/BPU. The number (x) in the front indicated the weight content of AlPU component. AlPU/APU as above.

Equations section

The tensile strength (σ_s) and elongation at break (e) of AlPU/BPU materials could be regarded as the summative contributions of two components (AlPU and BPU). We found that such relationship could be well fit by the linear equation in the form as:

$$\sigma_s = f_1 * x + f_2 * y + c \quad (1)$$

$$e = f_3 * x + f_4 * y + d \quad (2)$$

Where, x represents the mass fraction of AlPU in the PUE material, y represents the mass fraction of BPU in the PUE materials (x + y = 1. f_1, f_2, f_3 and f_4 are constant coefficients. c is a constant term).

We assumed that the tensile strength was composed of multiple stress factors corresponding to various components. And they might have the following linear relationship with the AlPU content:

$$\frac{\sigma}{f} = ax + b \quad (3)$$

Where σ denotes the actual tensile strength of the material, f denotes the stress factor simulated by molecular dynamics, and a, b are different constant coefficients, respectively.

Experimental information of characterization

Fourier transform infrared (FTIR) spectroscopy was conducted on a Thermo Scientific Nicolet iS20. Each spectrum was measured by 16 scans in a wavenumber range from 4000 cm^{-1} to 400 cm^{-1} at the resolution of 2 cm^{-1}.[1] The Gaussian peak splitting for analysing hydrogen bonding was performed by Origin 2021.

1H NMR spectra were monitored on a 400 NMR Bruker instrument (Bruker, German) at room temperature using DMSO-d6[2] solvents and NMR chemical shifts were reported in standard format as values in ppm relative to deuterated solvents.

Differential scanning calorimetry (TA DSC25) was used to characterize the thermal properties of AlPU/MPU materials under nitrogen flow. The temperature range was set to be from -80 °C to 150 °C and the heating rate was set to be 10

°C/min[3].

Small Angle X-ray Scattering (SAXS) was carried out on the Xeuss 2.0 (Xenocs, France). The wavelength of the radiation source was 1.54189 Å. In addition, the sample-to-detector distance was 1191.0 mm for SAXS. All the patterns were corrected for air scattering, background scattering, and beam fluctuations. The 2D SAXS radially integrated intensity $I(q)$ was obtained for integration in the azimuthal angular range of 0 - 360°. The long period (L) was calculated using the Bragg equation[4, 5]:

$$q = \frac{4\pi sin\theta}{\lambda} \quad (1)$$

Where q corresponds to the peak position in the scattering curves (i.e., $Iq2$ vs. q). The equatorial intensities were obtained by integration in the azimuthal angular range of -45° to 45° (the equatorial direction is along the stretching direction). In small-angle X-ray scattering (SAXS) analysis, the q value is a dimensionless quantity related to the scattering angle θ and wavelength λ of the X-rays. Therefore, the two-dimensional image of the SAXS axes is typically unitless. In addition, in SAXS analysis, the q value is a dimensionless relative scattering vector, independent of the distance from the sample to the detector, so the axes of the two-dimensional images do not need to be labeled with specific physical units. In SAXS analysis, the data are often normalized to the q-value, which facilitates comparisons between data from different experimental conditions without regard to the specific dimensions of the experimental setup. More importantly, since the q-value is not related to the specific size of the sample, but only to the scattering angle and wavelength of the X-rays, the use of the q-value rather than specific physical units of length allows for a wider range of applicability of SAXS data.

The mechanical properties of the samples were evaluated via tensile tests. The stress-strain curves were recorded at room temperature using an electronic universal tensile testing machine (UTM2102, Shenzhen Sanshi Zonghong Technology Co.) with a tensile speed of 20 mm/min[6]. All samples were cut into dumbbell-shaped specimens with the dimensions according to ISO 527-2/1BB (i. e., 50 mm's long and

4 mm's wide). At least five specimens were tested for each material to produce reliable results. The tensile strength was defined as the maximum stress divided by the initial cross-sectional area of the samples[7]. The toughness of all specimens was calculated by integrating the area under the stress-strain curves.

DFT calculations were carried out by the Gaussian 16 software[8]. The B3LYP functional was adopted for all calculations in combination with the D3BJ dispersion correction. In geometry optimization and frequency calculations, the 6-31G(d,p) basis set was used. The singlet point energy calculations were performed with a larger basis set combination, in which the ma-def2-TZVP basis set was used[9]. The SMD implicit solvation model was used to account for the solvation effect when performing single point energy calculations.

All-atom molecular dynamics (MD) simulations were performed using LAMMPS. The modelling uses the PCFF (Polymer Consistent Force Field) force field, and the modelling of molecular chains utilizes the Material Studio Build Polymer method. Two configurations of polymer chains were constructed separately, with n is 20 for the AIPU molecular chain and n is 20 for the MPU molecular chain. The model are converted into LAMMPS[3] data files for calculations. Different numbers of polymer chains are filled into a large box of dimensions 20*20*20 nm. The system is run under the NVT ensemble at 400K for 500 ps, followed by a 500 ps run under the NPT ensemble at 400K.Subsequently, a 100 ps run under the NPT ensemble is performed to cool the system to 300K. At 300K and under zero pressure conditions, the system is further relaxed for 100 ps until reaching equilibrium. Then, the periodic box in the X-direction is subjected to stretching. The stretching rate is 1e-6 1/fs. The stretching is sustained for 500 ps, resulting in a final strain of 1.0[10].

PALS (DPLS3000) were collected by a conventional fast-fast coincidence system with a time resolution (free width at half maximum, FWHM) of ~ 210 ps at room temperature. The positron source (22NaCl, sealed between two polyimide Kapton supporting foils in the size of 10 mm×10 mm×7.5 μm) was sandwiched between two identical samples with dimensions of 10×10×1 mm. The start and stop signals (γ rays of around 1.28 and 0.511MeV, respectively) were collected by two

detectors. To prevent backscattering of γ rays, the two detectors were perpendicularly positioned. The distance between the sample-source-sample set and the two lifetime detectors was around 20 mm. The total count of each PALS was 2.0 * 10^6, with a count rate of around 300 counts/s. The source correction (positron annihilation in 22NaCl and two polyimide Kapton supporting foils) was determined by the measurement of two identical YSZ (ZrO) samples in the size of 10×10×1 mm[7, 11].

Supplementary Figures

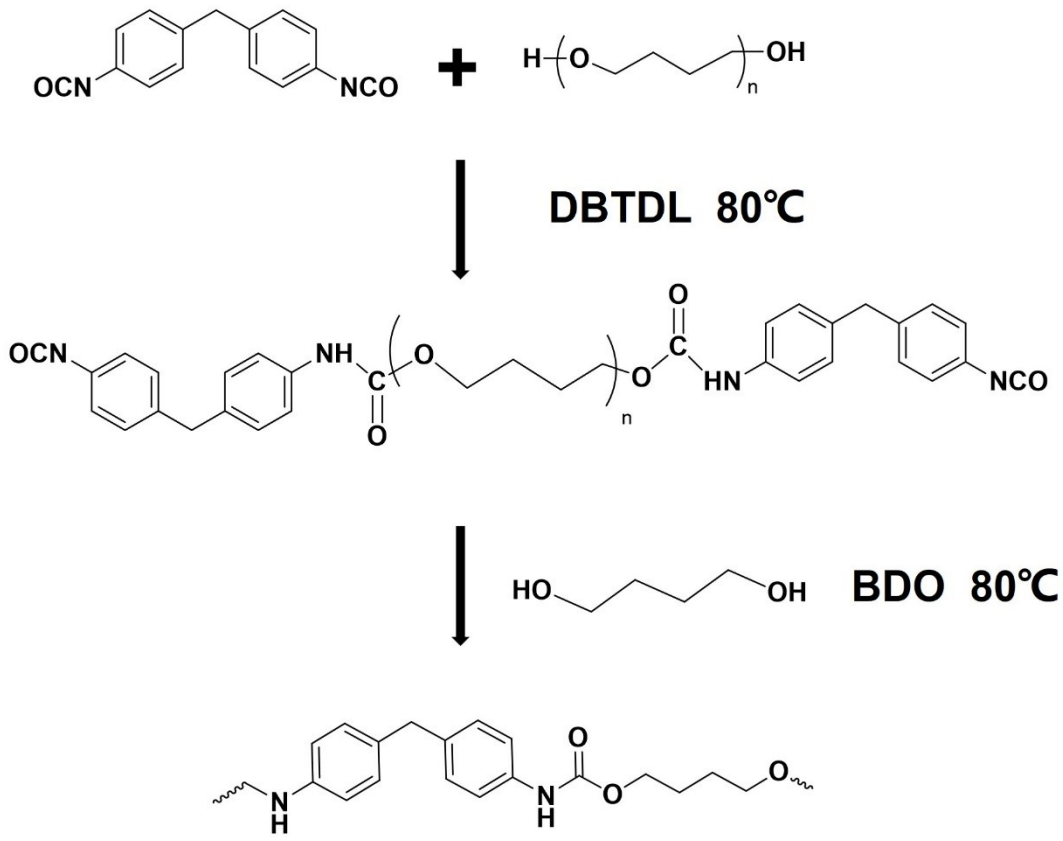

Figure S1. Synthetic procedure of the MPU material.

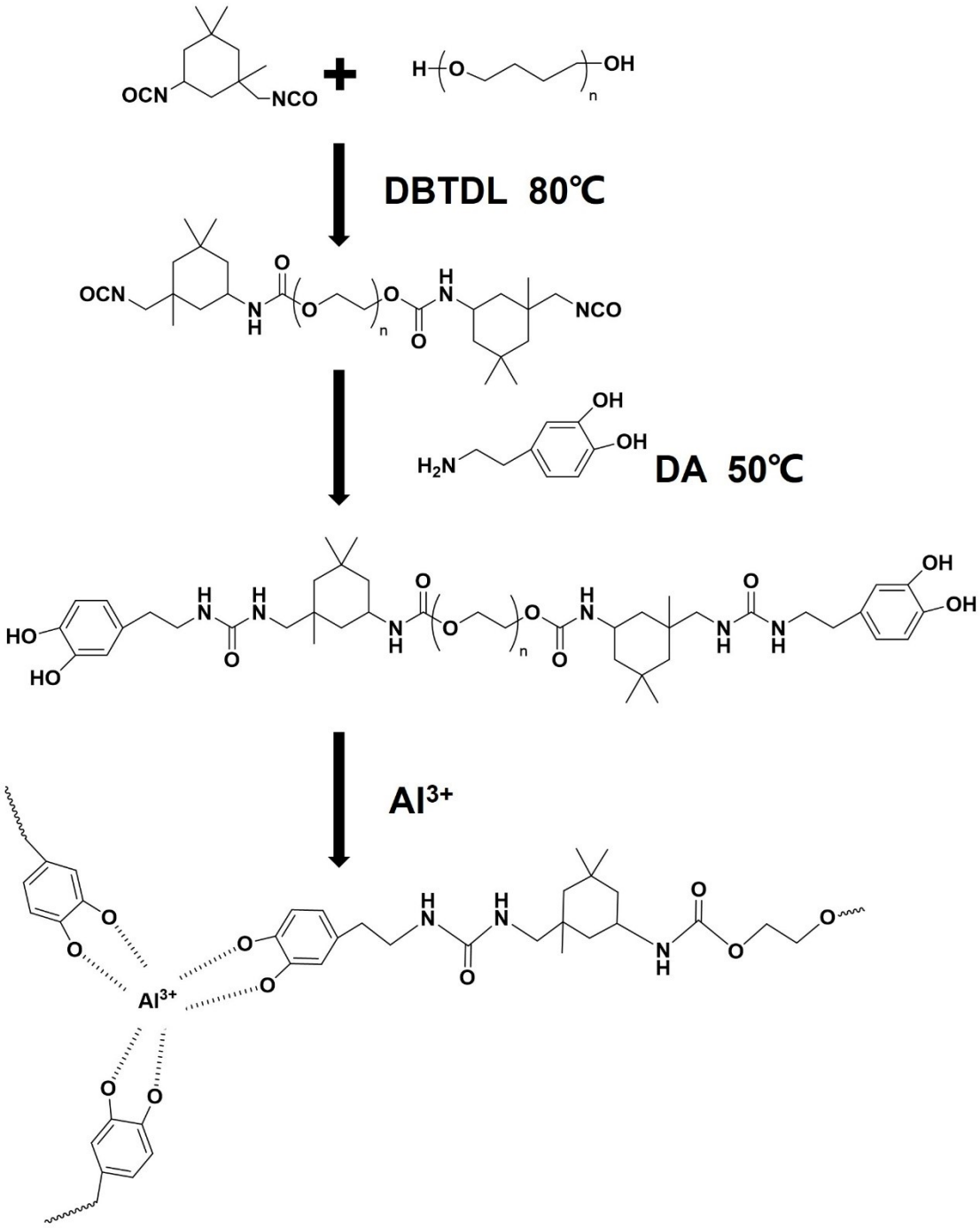

Figure S2. Synthetic procedure of the AlPU material.

Figure S3. A photograph of the FePU/MPU material.

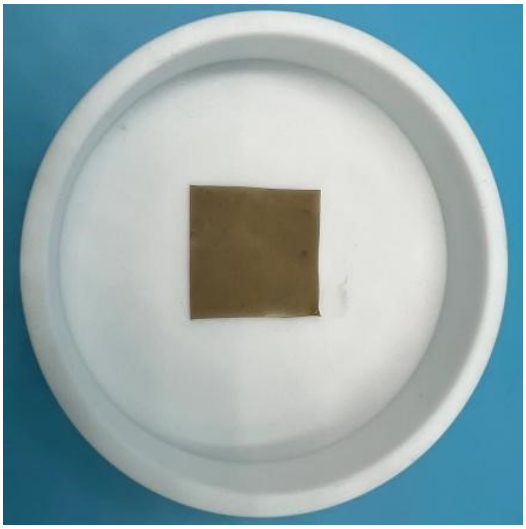

Figure S4. A photograph of the NiPU/MPU material.

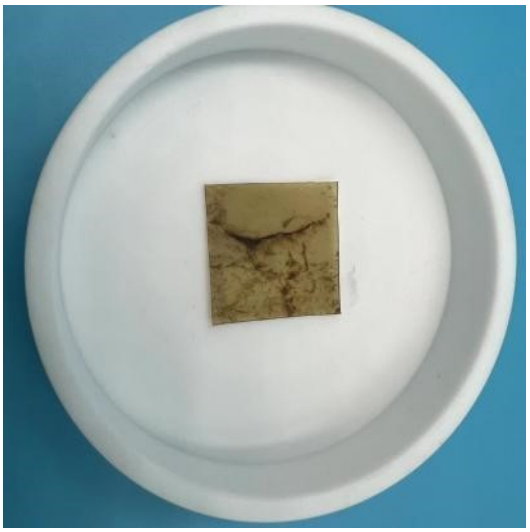

Figure S5. A photograph of the CaPU/MPU material.

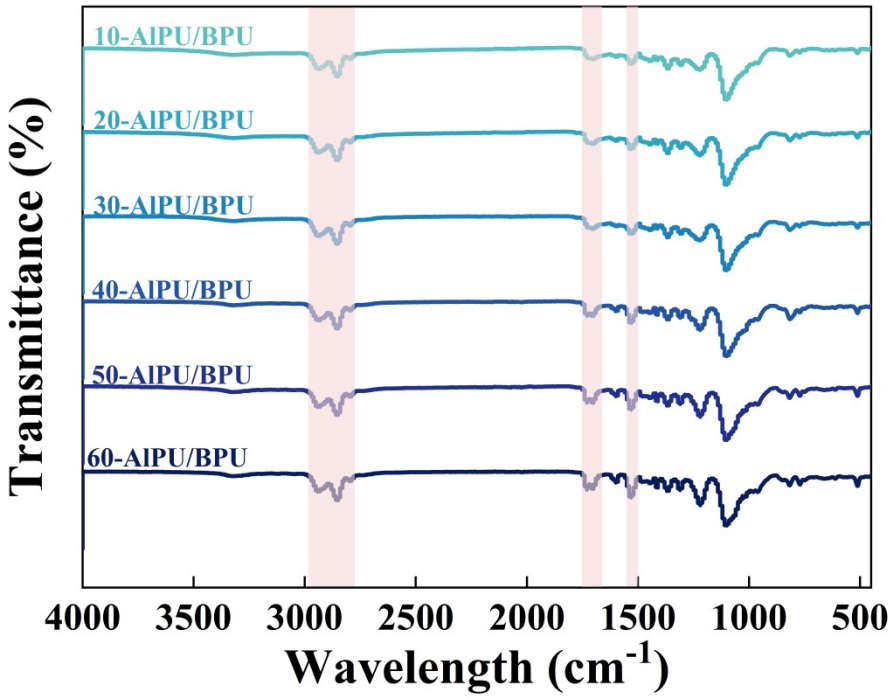

Figure S6. FTIR curves for diverse AlPU/BPU materials.

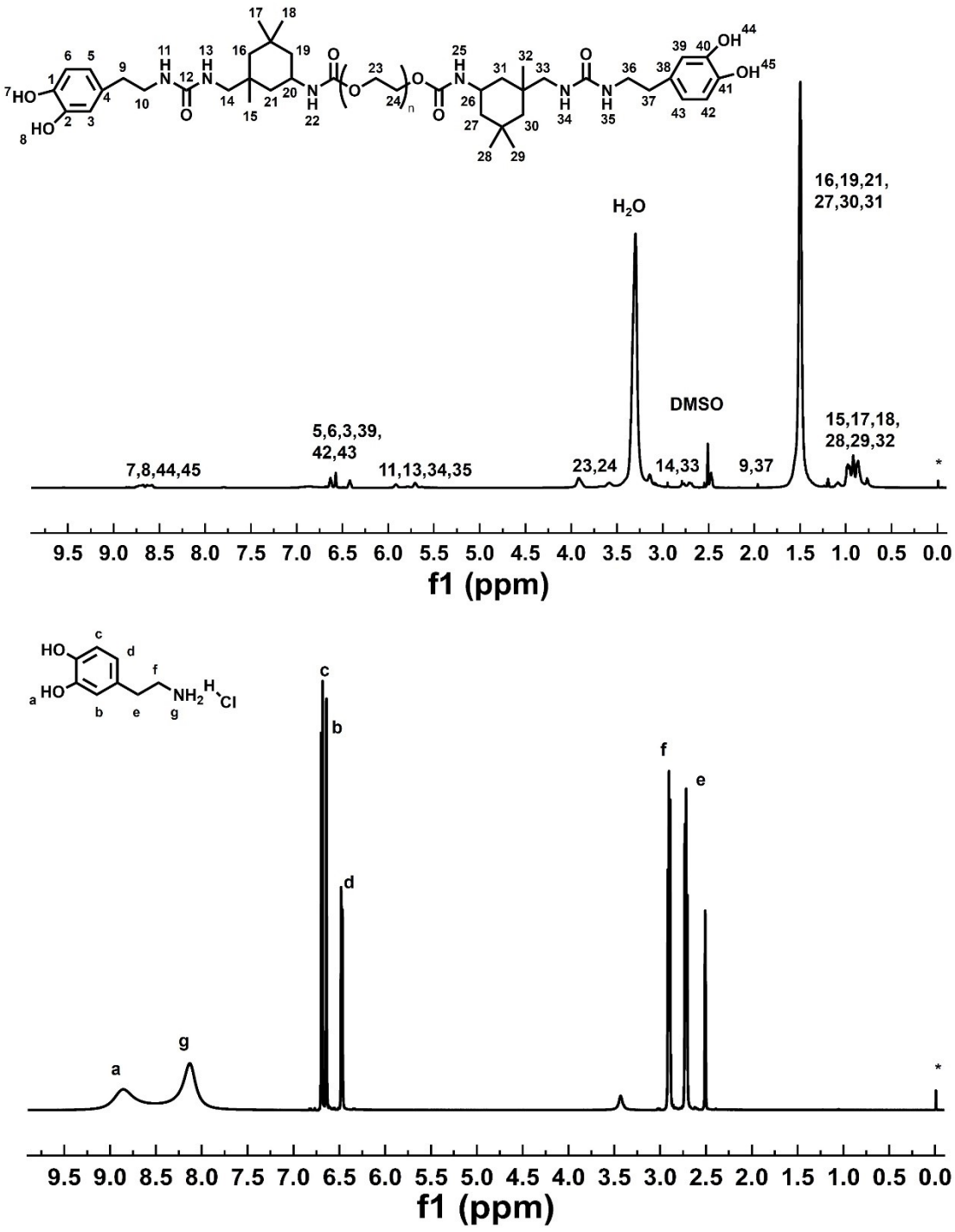

Figure S7. ^{1}H nuclear magnetic spectrum (400 MHz, $(CD_3)_2SO$, 298k) of DAPU and DA.

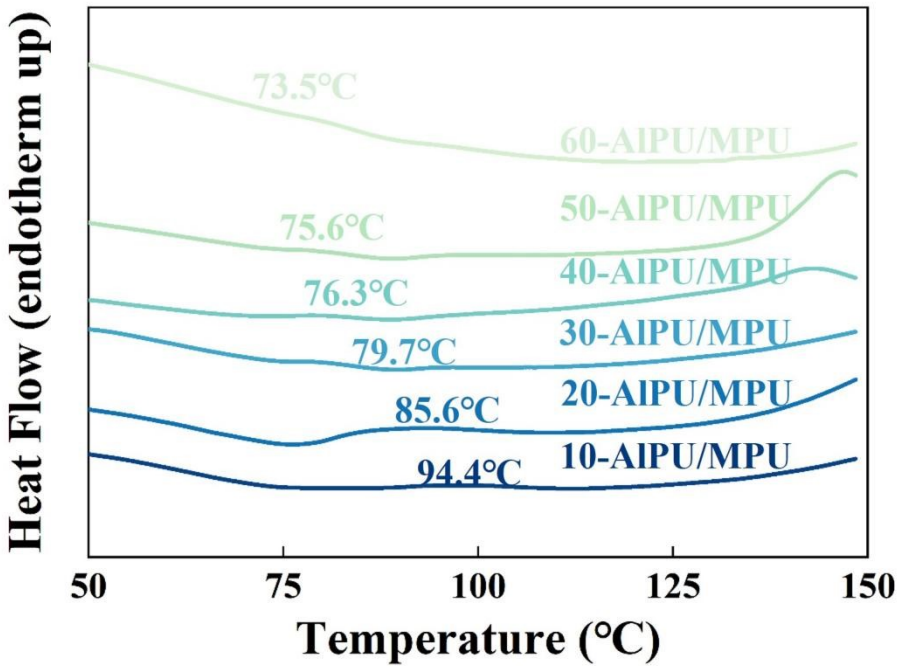

Figure S8. DSC curves for AlPU/MPU

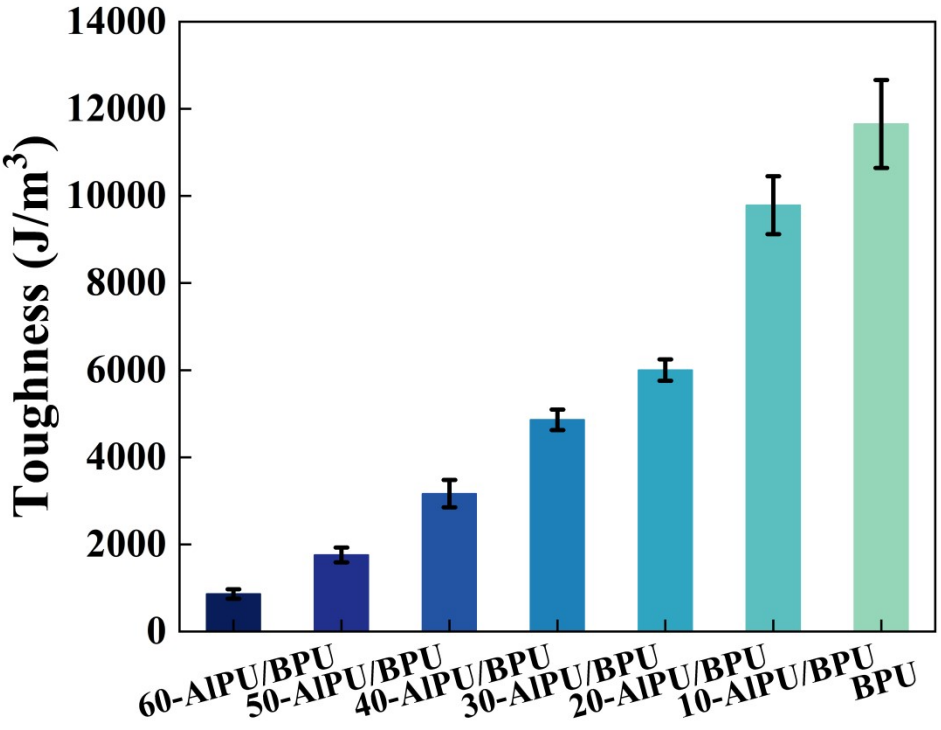

Figure S9. Statistic data for the toughness of diverse AlPU/MPU materials.

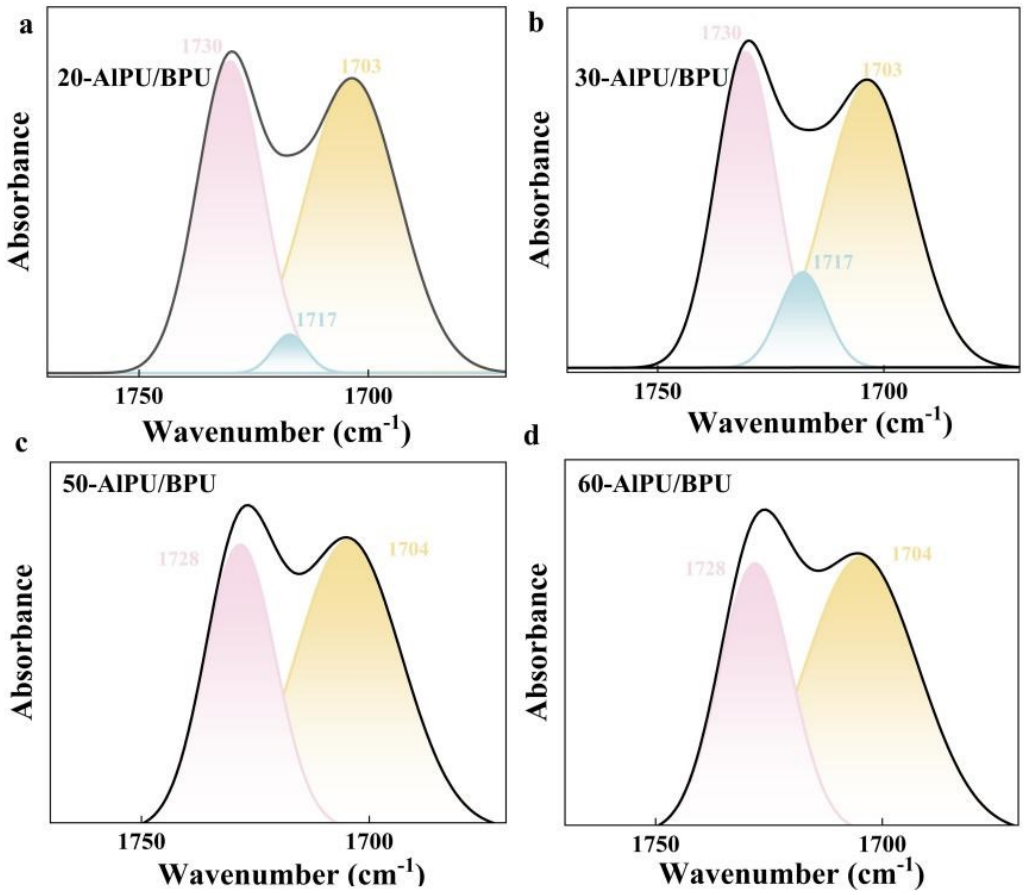

Figure S10. Gaussian infrared C=O peak splitting for (a) 20-AlPU/BPU, (b) 30-AlPU/BPU, (c) 50-AlPU/BPU and (d) 60-AlPU/BPU respectively.

The attribution of infrared spectra bands for stretching vibration of C=O groups in diverse AlPU/MPU materials via Gaussian peak separation. The peak at 1730 cm^{-1}-1735 cm^{-1} corresponded to the free hydrogen-bonded, the peaks at 1695 cm^{-1}-1704 cm^{-1} represent ordered hydrogen bonding C=O groups, while the one at 1716 cm^{-1}-1722 cm^{-1} represent disordered hydrogen bonding C=O groups.

By processing the curves, we have carefully delineated the C=O absorption peaks (1650-1750 cm^{-1}) for further processing and analysis. FTIR spectroscopy was an effective means to analyse the characteristics of ordered hydrogen bonding, and the range of C=O ordered hydrogen bonding is between 1695-1704 cm^{-1}. It was worth noting that the carbonyl absorption peaks might change slightly under the influence of ureido or carbamate groups, and the ordered hydrogen bonding absorption peaks might change slightly depending on the raw materials of polyurethane hard or soft segments, but the changes of ordered hydrogen bonding intervals did not change

significantly due to the above reasons.

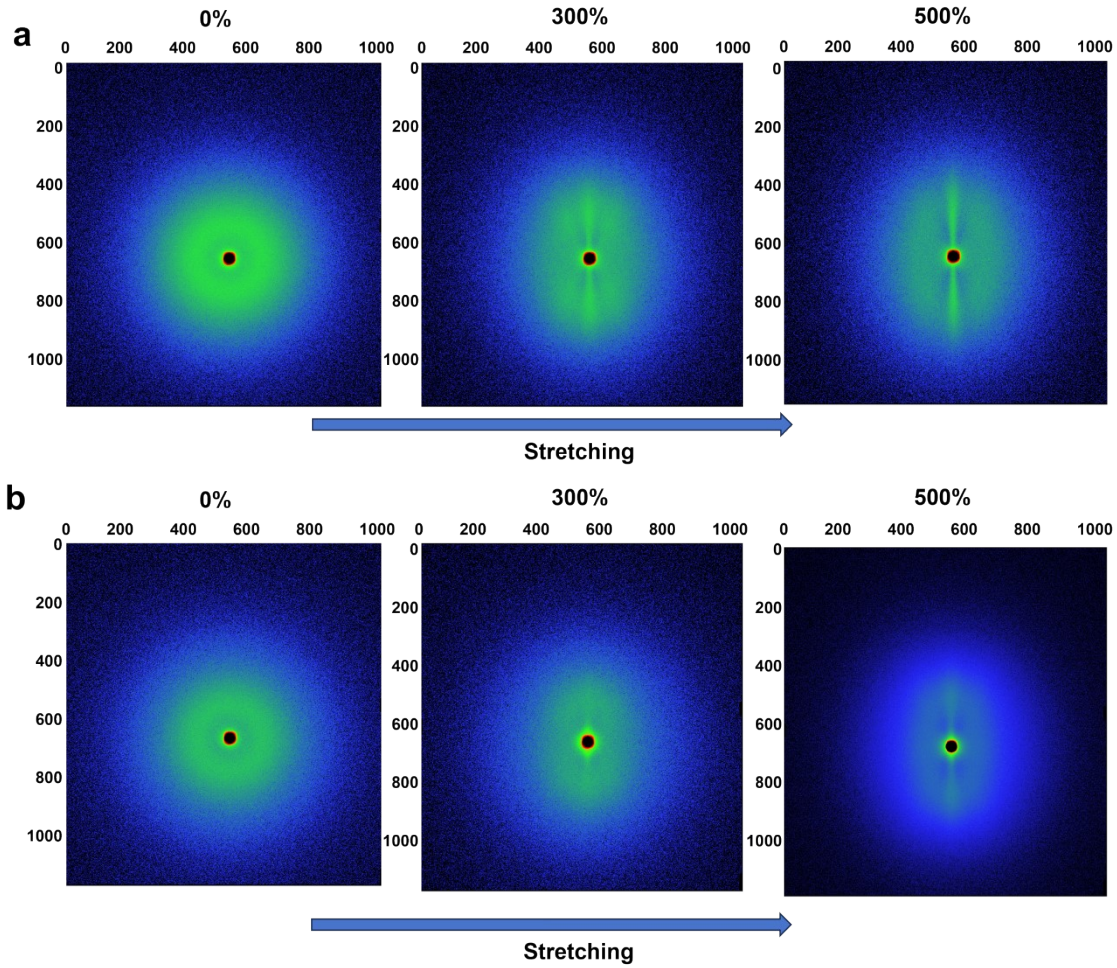

Figure S11. 2D SAXS patterns of the AlPU (a) and BPU (b) elastomer upon stretching.

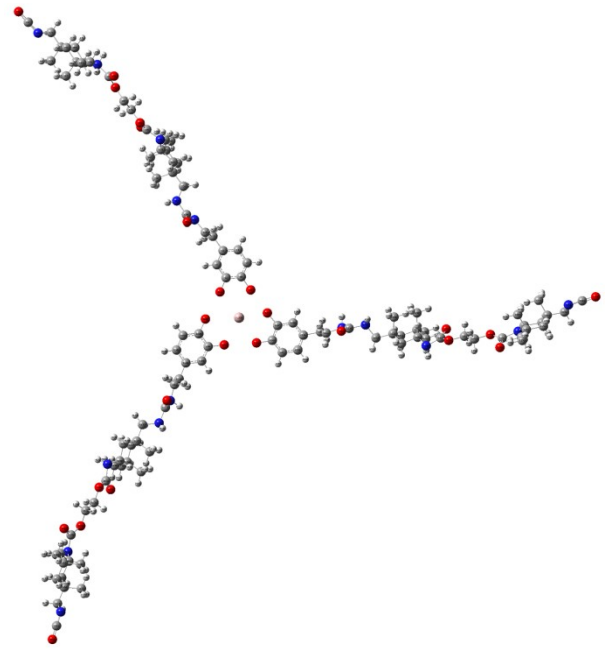

Figure S12. The density functional calculation models for AlPU.

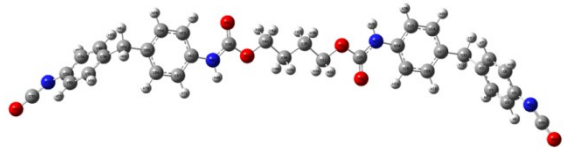

Figure S13. The density functional calculation models for BPU.

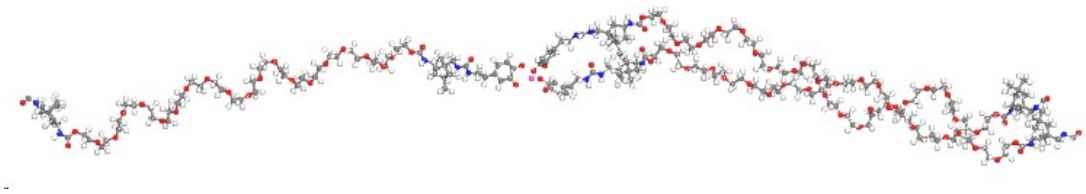

Figure S14. The all-atom molecular dynamics (MD) simulations models for AlPU.

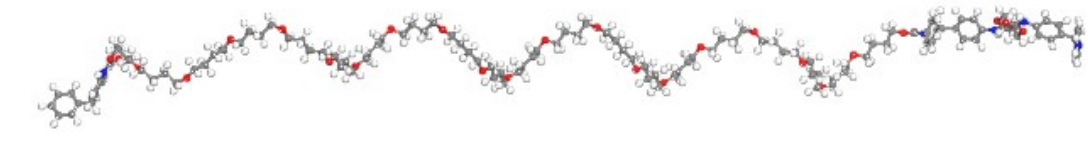

Figure S15. The all-atom molecular dynamics (MD) simulations models for BPU.

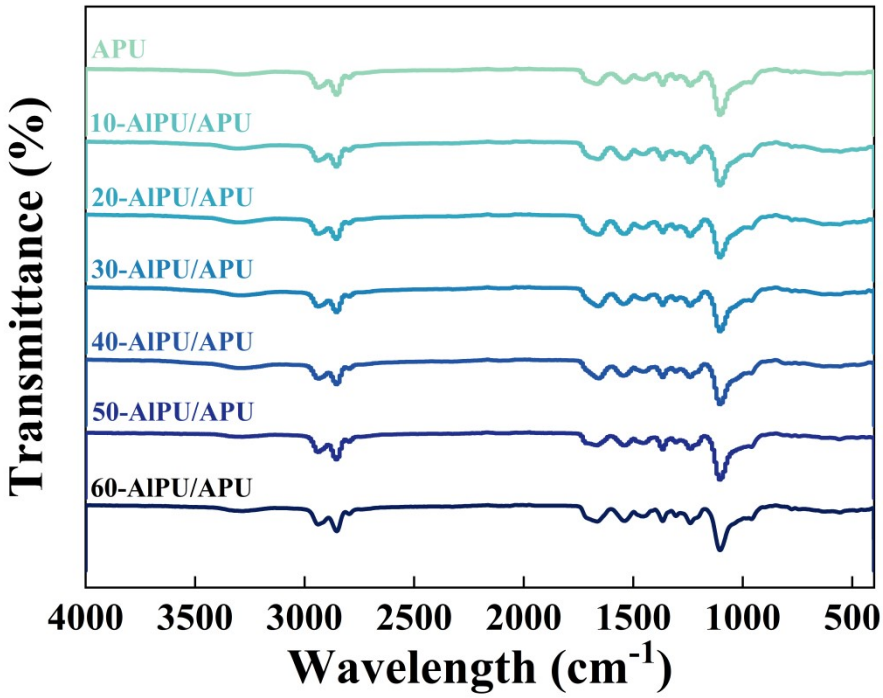

Figure S16. FTIR curves for diverse AlPU/APU materials.

Supplementary Tables

Table S1. Composition of the AlPU/BPU samples

Sample	AlPU (g)	BPU (g)	Total mass (g)
60-AlPU/BPU	9	6	15
50-AlPU/BPU	7.5	7.5	15
40-AlPU/BPU	6	9	15
30-AlPU/BPU	4.5	10.5	15
20-AlPU/BPU	3	12	15
10-AlPU/BPU	1.5	13.5	15
BPU	0	15	15

Table S2. Composition of the AlPU/APU samples

Sample	AlPU (g)	APU (g)	Total mass (g)
60-AlPU/APU	9	6	15
50-AlPU/APU	7.5	7.5	15
40-AlPU/APU	6	9	15
30-AlPU/APU	4.5	10.5	15
20-AlPU/APU	3	12	15
10-AlPU/APU	1.5	13.5	15
APU	0	15	15

References

1. M. W. M. Tan, H. Bark, G. Thangavel, X. Gong and P. S. Lee, *Institute for Chemical Reaction Design and Discovery (WPI-ICReDD), Hokkaido University, N21W10, Kita-ku, Sapporo, 001‐0021, Japan;Faculty of Advanced Life Science, Hokkaido University, N21W11, Kita-ku, Sapporo, 001-0021, Japan;Grad*, 2022, **13**.

2. Z. Weng, X. Huang, S. Peng, L. Zheng and L. Wu, *Institute for Chemical Reaction Design and Discovery (WPI-ICReDD), Hokkaido University, N21W10, Kita-ku, Sapporo, 001‐0021, Japan;Faculty of Advanced Life Science, Hokkaido University, N21W11, Kita-ku, Sapporo, 001-0021, Japan;Grad*, 2023, **14**.

3. X. Zheng, Y. Jia and A. Chen, *Institute for Chemical Reaction Design and Discovery (WPI-ICReDD), Hokkaido University, N21W10, Kita-ku, Sapporo, 001‐0021, Japan;Faculty of Advanced Life Science, Hokkaido University, N21W11, Kita-ku, Sapporo, 001-0021, Japan;Grad*, 2021, **12**.

4. J. Xu, X. Wang, X. Zhang, Y. Zhang, Z. Yang, S. Li, L. Tao, Q. Wang and T. Wang, *Chemical Engineering Journal*, 2023, **451**.

5. J. Wu, J. Deng, G. Theocharidis, T. L. Sarrafian, L. G. Griffiths, R. T. Bronson, A. Veves, J. Chen, H. Yuk and X. Zhao, *Nature*, 2024, **630**, 360-367.

6. Z. Ping, F. Xie, X. Gong, F. Zhang, J. Zheng, Y. Liu and J. Leng, *Advanced Functional Materials*, 2024, DOI: 10.1002/adfm.202402592.

7. M. Deng, Y. Ding, Z. He, B. Shan, X. Cao and B. Tang, *Construction and Building Materials*, 2021, **278**.

8. Z. Li, Z. Hou, H. Fan and H. Li, *Advanced Functional Materials*, 2016, **27**.

9. Z. H. Zhao, S. Y. Chen, P. C. Zhao, W. L. Luo, Y. L. Luo, J. L. Zuo and C. H. Li, *Angew Chem Int Ed Engl*, 2024, **63**, e202400758.

10. W. Li, H. Wu, Y. Huang, Y. Yao, Y. Hou, Q. Teng, M. Cai and J. Wu, *Angew Chem Int Ed Engl*, 2024, DOI: 10.1002/anie.202408250, e202408250.

11. X. Chen, X. Li, H. Zhang, H. Li, G. Wang and Y. Cui, *Macromolecules*, 2023, **Vol.56**, 8993-9002.